

Evolution in the Electronic Structure of Polymer-derived Amorphous Silicon Carbide

Kewei Wang,^{‡,§} Xuqin Li,^{‡,§} Baisheng Ma,^{‡,§} Min Zhang,[‡] Jinling Liu,[‡] Yiguang Wang,^{‡,§} Ligong Zhang,[¶] and Linan An^{||,†}

[‡]State Key Laboratory of Solidification Processing, Northwestern Polytechnical University, Xi'an, Shaanxi 710072, China

[§]Science and Technology on Thermostuctural Composite Materials Laboratory, Northwestern Polytechnical University, Xi'an, Shaanxi 710072, China

[¶]State Key Laboratory of Luminescence and Applications, Changchun Institute of Optics, Fine Mechanics and Physics, Chinese Academy of Sciences, Changchun, China

^{||}Department of Materials Science and Engineering, Advanced Materials Processing and Analysis Center, University of Central Florida, Orlando, Florida 32816

The electronic structure of polymer-derived amorphous silicon carbide pyrolyzed at different temperatures was investigated by combining measurements of their temperature-dependent conductivity and optical absorption. By comparing the experimental results with theoretical models, the parameters such as conduction band, band-tail, defect energy, and Fermi energy were determined. The results revealed that band gap and band-tail width decreased with increasing pyrolysis temperature. Furthermore, it was found that electrons transport followed a band-tail hopping mechanism, rather than variable range hopping. These results were discussed in accordance with the microstructural evolutions of the material.

I. Introduction

AMORPHOUS silicon-based ceramics synthesized by thermal decomposition of polymeric precursors (referred to as polymer-derived ceramics, PDCs) have received extensive attention in recent years due to their unique processing, structures, properties, and potential applications at high temperatures. As compared to polycrystalline ceramics, one distinguished feature of PDCs is that their structures and properties changed significantly with synthesis temperature (namely, material evolution), likely due to their amorphous nature. This phenomenon is rather remarkable since it not only provided a fruitful testing system for learning fundamental sciences in non-oxide amorphous solids, but also offered a convenient way to tailor material properties for various applications.

Consequently, material evolution of PDCs has been the focus of numerous publications in the past years. These work depicted rather clear pictures of the evolutions of the network structures^{1–8} and electric properties^{9–16} of the materials. However, the evolution of the electronic structures of PDCs has been ignored. Such “negligence” is rather unconscionable, given that PDCs exhibited unique high-temperature semiconducting behavior^{17,18} and are promising for making high-temperature microelectromechanical systems and microsensors.^{19–22} Learning their electronic structure evolutions can lead to a better understanding of the semiconducting

behavior and form a guideline for the applications of the materials. One reason that is responsible for the “negligence” is that the electronic structure of amorphous semiconductors is rather complex and difficult for theoretical calculation; and the complex structures and compositions of PDCs made the situation even worse. Recently, Wang and co-workers have determined the electronic structure of a PDC by combining optical absorption measurement and temperature-dependent conductivity measurement.²³ The electronic structural parameters (including bandgap, band-tail, defect energy level, and Fermi energy level) were measured by the technique. More importantly, this work provided a useful tool to experimentally determine the electronic structures of PDCs.

In this study, we report a detailed study on the effect of the pyrolysis temperature on the electronic structure of a polymer-derived amorphous silicon carbide (*a*-SiC). We show that the optical bandgap, band-tail, and defect level are all significantly varied with pyrolysis temperature. We also reveal that the material exhibits unique electronic structure where the band-tail and defect level overlap with each other, which leads to a band-tail hopping process. The unique characteristics and evolution of the electronic structure of the material are rationalized according to its network structure and processing.

II. Experimental Procedure

The *a*-SiC ceramics studied here were prepared by pyrolyzing a polycarbosilane provided by Xiamen University.^{12,24} The as-received liquid precursor was first cross-linked at 150°C for 2 h and 400°C for 1 h in ultrahigh purity argon environment. The resultant solid was ground to fine powder of ~1 μm using high-energy ball-milling. The powder was then pressed into disks of 16 mm in diameter and 1 mm in thickness at a uniaxial pressure of 50 MPa followed by cold isostatic pressing at 200 MPa for 5 min. The disks were finally pyrolyzed at different temperatures of 1000°C, 1100°C, 1200°C, and 1300°C for 4 h under the protection of flowing ultrahigh purity argon. The obtained materials were amorphous with the composition of ~SiC_{1.45}O_{0.08}, independent of pyrolysis temperature; the small amount of oxygen is likely due to the contamination during material synthesis.¹²

For electric conductivity measurement, the specimens were first polished to 1 μm finish. Silver paste was painted on the surfaces of the samples as the electrodes. The temperature-dependent electrical conductivity of the samples is then measured in a tube furnace under flowing ultrahigh purity nitrogen. To obtain the accurate temperatures, a thermal

R. Riedel—contributing editor

couple is placed just above the samples. The measurement was conducted by measuring the I - V curve on Agilent 4155C semiconductor parameter analyzer (Agilent Technologies, Inc., Santa Clara, CA) at the temperature range 50°C–650°C.²⁵

To obtain the meaningful data, the optical absorption was measured on the same sample used for conductivity measurement to avoid variations from sample to sample (which is normally the case for PDCs). To do so, the sample used for was grinded to powder of ~ 1 μm after the conductivity measurement. The powder was then mixed with KBr powder and pressed into a disk of 10 mm diameter and 0.5 mm thick. The ratio of the a -SiC powder to the KBr powder was tailored to maintain the overall absorption coefficient between 0.2 and 0.8 for the best results. The optical absorption spectra were obtained on a UV-3101 double channel spectrometer (Shimadzu Co., Kyoto, Japan).¹⁵

III. Results

Figure 1(a) shows the optical absorption coefficient (α) as a function of photon energy ($h\nu$) for the four samples. It is seen that the a -SiC exhibited absorption over entire phonon energy range between 1.5 and 5 eV, which is a typical behavior of amorphous semiconductors. Previous study showed that amorphous semiconductors should exhibit a direct optical transition between the two delocalized bands.^{26,27} This absorption can be used to determine the absorption edge according to the following equation:

$$(\alpha h\nu)^2 \propto (h\nu - E_g) \quad (1)$$

where E_g is optical bandgap between conduction band (E_C) and valence band (E_V). Figure 1(b) replots the raw data shown in Fig. 1(a) in the format of $(\alpha h\nu)^2$ versus $h\nu$. The bandgaps are then estimated by extrapolation of the linear portion of the curves in high photon energy ranges [dashed lines in Fig. 1(b)]. The obtained bandgaps for the four a -SiC ceramics are listed in Table I, which are within the same range as those measured from a -SiC thin films synthesized by vapor deposition.²⁸

Figure 1 reveals that the absorption coefficient within lower phonon energy range is not zero, suggesting that there should be other absorption mechanisms in addition to the transition between the extended bands. Previous studies suggested that there was a so-called Tauc absorption for amorphous semiconductors at a lower excitation energy range. This absorption can be described by Ref. [29–31].

$$\alpha h\nu = B(h\nu - E_T)^n \quad (2)$$

where n is a constant, E_T an energy gap (named Tauc bandgap), and B a constant. According to Inkson,³² Tauc absorption is resulted from a transition between deep impurity trap and

Table I. Fitting Parameters for the Optical Absorption Curves

Pyrolysis temperature(°C)	E_g (eV)	E_T (eV)	n	χ_1^2
1000	3.25	0.49	1.48	5.5×10^{-6}
1100	3.19	0.37	1.46	2.5×10^{-7}
1200	2.75	0.35	1.53	4.5×10^{-7}
1300	2.70	0.17	1.50	1.6×10^{-6}

delocalized band (either conductive or valence band). Pfost et al. suggested that Tauc bandgap could be related to the electronic structures of amorphous semiconductors; when $n \sim 1.5$,³³

$$E_T = E_C - E_D \quad (3)$$

where E_D is a deep defect level with a high density of state. To determine if there is Tauc transition in our materials, the absorption behavior of the a -SiC is measured in the excitation energy range 0.5–1.0 eV. Figure 2 compares the experimental data with Eq. (2). The good agreement between the two confirms the existence of Tauc transition in our materials. The parameters used for achieving the best fit in Fig. 2 and deviance χ_1^2 are listed in Table I. It is seen that the n values are close to 1.5, suggesting that the transition is between the deep defect states and the mobility edge.

Figure 3 shows the temperature-dependent conductivity for the materials pyrolyzed at different temperatures. The conductivity increases with increasing pyrolysis temperature, consistent with all previous observations for polymer-derived amorphous ceramics. The increase in the conductivity as increasing testing temperature indicates that all materials exhibit semiconducting behavior. The dependence of the conductivity on testing temperature decreases with increasing pyrolysis temperature, suggested by the decrease in the slope of the curves in Fig. 3.

It is known that three conduction mechanisms can occur in an amorphous semiconductor. The temperature-dependent conductivity of an amorphous semiconductor can be described by the following equation:³⁴

$$\sigma = \sigma_1 e^{-\frac{E_C - E_F}{kT}} + \sigma_2 e^{-\frac{E_A - E_F + w}{kT}} + \sigma_3 e^{-(\frac{T_0}{T})^{1/4}} \quad (4)$$

where E_C , E_A , and E_F are the mobility edge for conduction band, band-tail, and Fermi level, respectively; w the thermal activation energy, which is equal to the phonon energy of the material (here we assume that the phonon energy of the a -SiC is equal to that of crystalline SiC, which is 100 meV³⁵); σ_1 , σ_2 , and σ_3 prefactors without clear physical meaning; and T_0 a characteristic temperature. The first term in the equation is the contribution from the conduction in extended states, which is the dominate mechanism at high temperatures;

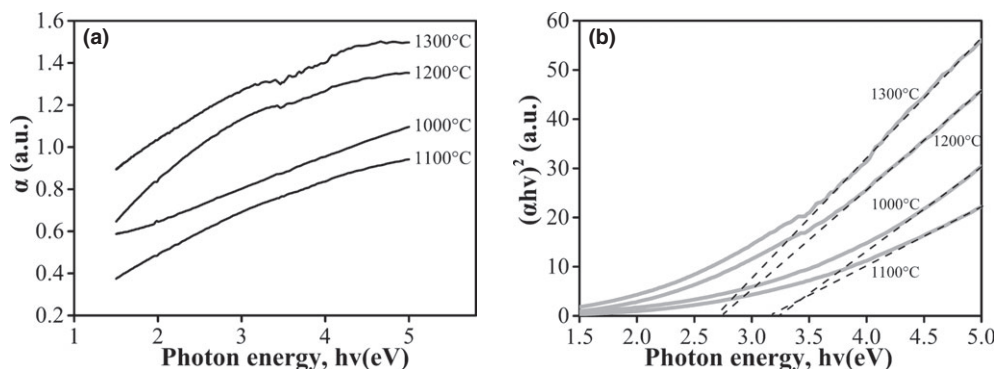


Fig. 1. (a) The raw data of the absorption coefficient as a function of photon energy for the a -SiC pyrolyzed at different temperatures as labeled; and (b) a plot of $(\alpha h\nu)^2$ as a function of photon energy, the band gaps for the a -SiC ceramics can be estimated by extrapolation (dashed lines).

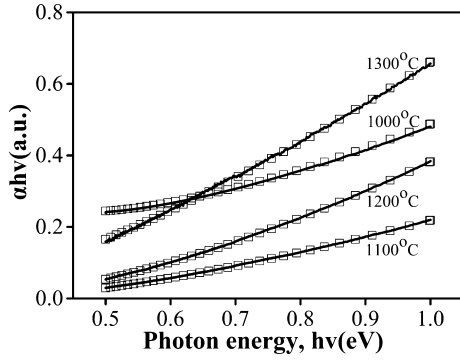


Fig. 2. A plot of αhv as a function of the photon energy for the four a -SiC as labeled. The data points are measured experimentally and the solid lines are computed from Eq. (2).

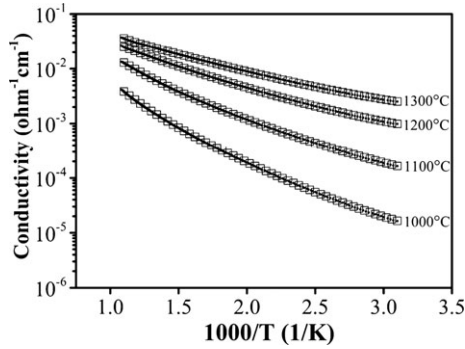


Fig. 3. Plots of the electrical conductivity as a function of testing temperature for the a -SiC synthesized at different pyrolysis temperature as labeled. The open squares are the experimental data; and the solid lines are computed from Eq. (4).

the second term is the contribution from the conduction in band-tail states, which is the dominate mechanism at middle temperatures; and the third term is the contribution from the conduction in localized states, which is the dominate mechanism at low temperature. The experimental data were compared with Eq. (4) (Fig. 3) for the four samples. The excellent agreement between the experimental data and those computed from Eq. (4) suggests that the conduction behavior of the materials can be described by the equation. The important fitting parameters from the best curve-fitting and deviance χ_2^2 are listed in Table II.

The electronic structures of the a -SiC ceramics can then be determined from the data in Tables I and II by following the procedure below:

1. The conduction edge (E_C) is determined from the measured bandgap ($E_C = E_g + E_V$) by assuming that the valence band edge to be zero.
2. The band-tail edge (E_A) is determined by using the following equation (where w is 100 eV): $E_A = E_C - (E_C - E_A) = E_C - [(E_C - E_F) - (E_A - E_F + w)] - w$.
3. Fermi energy (E_F) is determined by $E_F = E_C - (E_C - E_F)$.
4. Defect energy (E_D) is determined by $E_D = E_C - E_T$.

The obtained electronic structures are schematically drawn in Fig. 4. The figure clearly shows that the electronic structure of the a -SiC are significantly influenced by pyrolysis temperature.

IV. Discussion

Electronic structures were determined for the polymer-derived a -SiC ceramics prepared at different pyrolysis temperatures by combining measurements on their temperature-dependent conductivity and optical absorption. It can be seen clearly from Fig. 4 that the pyrolysis temperature has profound effects on the structures. In this section, we shall discuss these effects in details and correlated the changes in electronic structures to the changes in network structures of the materials.

(1) Effect on Bandgap

Previous study on the structures of the a -SiC ceramics revealed that the materials have a Si-based phase and a free carbon phase.²⁴ The Si-based phase is an amorphous network comprised of SiC_4 tetrahedra and a small amount of $\text{SiC}_x\text{O}_{4-x}$ tetrahedra. The measured band gaps, thus, should reflect the optical absorption by the amorphous SiC_4 network. Previous study revealed that the band gap of amorphous SiC could vary between 2.0 and 3.6 eV, depending on the concentrations of carbon and hydrogen.²⁸ It is seen that the values measured for the polymer-derived a -SiC indeed fall in this range, confirming that the optical absorption of the current materials are from the SiC_4 network.

Figure 5 plots the bandgap as a function of pyrolysis temperature for the four materials. It is seen that the bandgap decreases with pyrolysis temperature, with a sudden change between 1100°C and 1200°C. Studies on a -SiC thin films synthesized by vapor deposition revealed that the bandgap of this type of material can be drastically affected by Si:C ratio and hydrogen concentration: increasing carbon concentration leads to an increase in the bandgap,^{28,36,37} and hydrogen can also widen the bandgap.^{38,39} Previous study²⁴ on the network structure of this a -SiC revealed that the material does contain a small amount of extra carbon more than the necessary to form stoichiometric SiC within the Si-containing phase. However, the concentration of the carbon and the composition of the samples remained the constant within the testing temperature range,²⁴ indicating the bandgap change was not from the decrease in the carbon concentration.

It is well-known that with increasing pyrolysis temperature, the hydrogen concentration within PDCs decreases.^{13,40,41} Thereby, it is believed that the bandgap decrease with pyrolysis temperature in this study is mainly due to the loss of the hydrogen with increasing pyrolysis temperature. The sudden drop in the bandgap between 1100°C and 1200°C suggests the significant hydrogen loss within the temperature range.

(2) Effect on Band-Tail

The change in the width of the band-tail ($=E_C - E_A$) with pyrolysis temperature is illustrated in Fig. 6. Again, the band-tail width decreases with pyrolysis temperature, with a sudden change between 1200°C and 1300°C.

Table II. Fitting Parameters for the Conductivity Curves

Pyrolysis temperature (°C)	$E_C - E_F$ (eV)	$E_A - E_F + w$ (eV)	T_0 (K)	σ_3 ($/\Omega/\text{cm}$)	χ_2^2
1000	0.56	0.24	1.21×10^6	2.14×10^{-2}	6.9×10^{-7}
1100	0.49	0.20	2.38×10^5	1.50×10^{-2}	5.8×10^{-7}
1200	0.45	0.17	3.02×10^4	1.18×10^{-2}	5.4×10^{-7}
1300	0.20	0.12	9.37×10^3	9.52×10^{-3}	6.1×10^{-7}

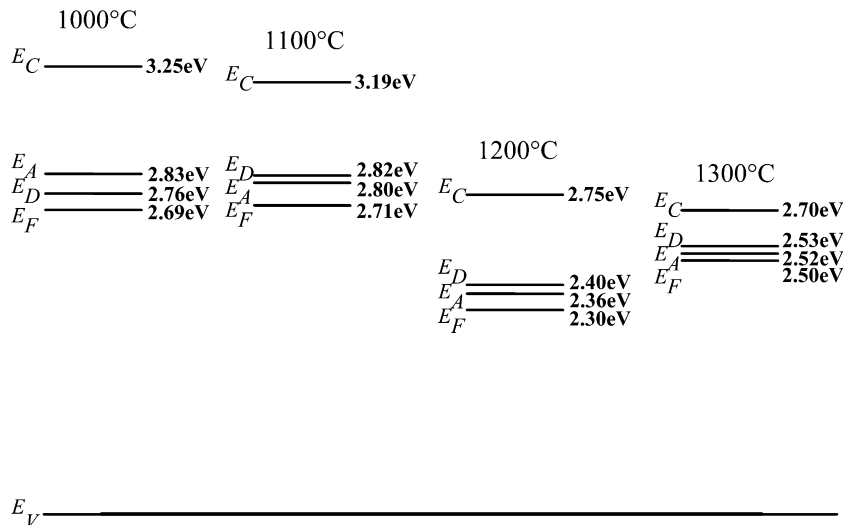


Fig. 4. A schematic showing the electronic structures of the amorphous SiC pyrolyzed at different temperatures.

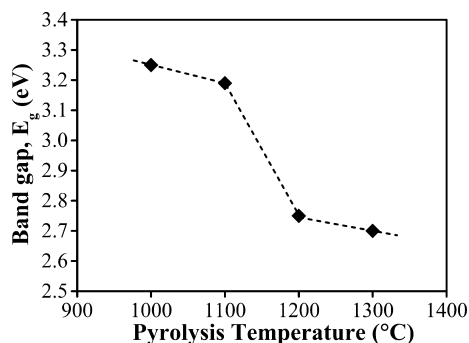


Fig. 5. A plot of the band gap as a function of pyrolysis temperature.

It is known that the existence of the band-tail is resulted from the deviation of an amorphous structure from periodic crystalline structure. For the same material, the band-tail width depends on the degree of order of the material. Decrease in the band-tail width suggests the increase in the degree of order. Previous study on the same material studied here revealed that the network structure of the material was becoming more order with increasing pyrolysis temperature,²⁴ consistent with the decrease in the band-tail width. More interestingly, it revealed that the material started to crystallize at $\sim 1250^\circ\text{C}$, suggesting there was a big change in the structure around this temperature; which consists with the sudden change in band-tail width between 1200°C and 1300°C .

(3) Hopping Mechanism

Previous studies revealed that there are two different electrons transport mechanisms in amorphous semiconductors at the low temperature range: one is variable range hopping (VRH) mechanism, in which electrons transport within the defect energy level close to the Fermi level,^{42,43} the other is band-tail hopping (BTH) mechanism, in which electrons within the defect level fill empty states near a so-called “transport energy” (within band-tail) and then hop back to lower localized states.^{44,45} The two processes lead to different relationships between the prefactor σ_3 and characteristic temperature T_0 . For VRH process, σ_3 and T_0 vary in opposite directions according to the following equation:⁴⁵

$$\sigma_3 \propto T_0^{-1/2} \quad (5)$$

While BTH process predicts that T_0 and σ_3 should obey the following relationship:^{44,45}

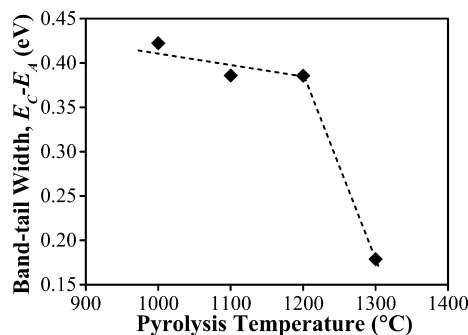


Fig. 6. A plot of band-tail width as a function of pyrolysis temperature.

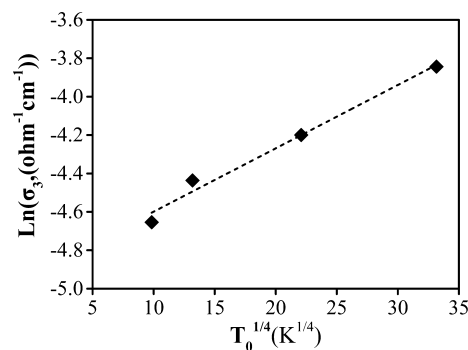


Fig. 7. A plot of prefactor σ_3 and characteristic temperature T_0 .

$$\ln \sigma_3 \propto T_0^{1/4} \quad (6)$$

Figure 7 plots the σ_3 vs. T_0 obtained from the current materials. It is seen that the relationship of the two parameters can be well described by Eq. (6), suggesting that the material follows BTH mechanism. This is consistent with the previous observation, which showed that PDCs followed BTH process.¹⁵

The material following BTH process rather than VRH process is likely related to their unique electronic structures. It can be seen from Fig. 4 that the band-tail edge, defect energy level and Fermi energy level are very close to each other in these materials; and for the materials obtained at temperatures 1100°C and above, the band-tails even extend into the defect energy level. Such structure provides a lot of

empty states with energy levels close to that of the defects; thus the transport of the defect electrons is rather via these states over via the states within defect level.

The overlap between the band-tail and the defect level is rather interesting; and is likely resulted from the unique synthesis procedure of PDCs. PDCs are synthesized by pyrolyzing the already cross-linked polymeric precursors at relative low temperatures. At such "low" temperatures, the covalent bond natured PDCs will have very low diffusion rates, making the atom rearrangements very difficult, which leads to two consequents: (i) the defects due to the decomposition-induced chemical bond broken are hard to be removed; and (ii) the network of the materials resulted from the "collapse" of the cross-linked polymer network has little chance to rearrange into a highly ordered manner. The combining effect of the wide band-tail resulted from highly disordered structure and the high defect energy level resulted from large amounts of point defects is likely responsible for the overlap.

V. Summary

Both room-temperature optical absorption and temperature-dependent conductivity were measured for the polycarbosilane-derived amorphous SiC ceramics prepared at different pyrolysis temperatures. The experimental results were compared with theoretical models to deduce the electronic structures of the materials. The results showed several unique features in the electronic structure and its evolutions with pyrolysis temperature. One remarkable feature of the electronic structures is that the band-tail and defect level overlap with each other, likely resulting from a relatively large amount of defects and high disordered structure of the materials. This feature explained band-tail hopping rather than variable-rang-hopping process observed in the materials. The bandgap of the material decreases with increasing pyrolysis temperature with a sudden drop between 1100°C and 1200°C, which was ascribed to the release of the residual hydrogen within the materials. In addition, the band-tail width of the material also decreases with pyrolysis temperature with a sudden drop between 1200°C and 1300°C, which was attributed to the increase in the degree of order of the amorphous network.

Acknowledgments

This work was financially supported by the Chinese Natural Science Foundation (grant no. 51372202), State Key Laboratory of Solidification Processing (grant no. 82-TZ-2013), and the "111" project (B08040).

References

- Y. Iwamoto, W. Völger, E. Kroke, R. Riedel, T. Saitou, and K. Matsunaga, "Crystallization Behavior of Amorphous Silicon Carbonitride Ceramics Derived from Organometallic Precursors," *J. Am. Ceram. Soc.*, **84** [10] 2170–8 (2010).
- G. Gregori, H.-J. Kleebe, H. Brequel, S. Enzo, and G. Ziegler, "Microstructure Evolution of Precursors-Derived SiCN Ceramics upon Thermal Treatment Between 1000 and 1400°C," *J. Non-Cryst. Solids*, **351** [16–17] 1393–402 (2005).
- J. Seitz, J. Bill, N. Egger, and F. Aldinger, "Structural Investigations of Si/C/N-Ceramics from Polysilazane Precursors by Nuclear Magnetic Resonance," *J. Eur. Ceram. Soc.*, **16** [8] 885–91 (1996).
- J. Haug, P. Lamparter, M. Weinmann, and F. Aldinger, "Diffraction Study on the Atomic Structure and Phase Separation of Amorphous Ceramics in the Si-(B)-C-N System. 1. Si-C-N Ceramics," *Chem. Mater.*, **16** [1] 72–82 (2004).
- J. Haug, P. Lamparter, M. Weinmann, and F. Aldinger, "Diffraction Study on the Atomic Structure and Phase Separation of Amorphous Ceramics in the Si-(B)-C-N System. 2. Si-B-C-N Ceramics," *Chem. Mater.*, **16** [1] 83–92 (2004).
- S. Widgeon, et al., "Nanostructure and Energetics of Carbon-Rich SiCN Ceramics Derived from Polysilylcarbodiimides: Role of the Nanodomain Interfaces," *Chem. Mater.*, **24** [6] 1181–91 (2012).
- Y. Gao, et al., "Effect of Demixing and Coarsening on the Energetics of Poly(Boro)Silazane-Derived Amorphous Si-(B)-C-N Ceramics," *Scripta Mater.*, **69** [5] 347–50 (2013).
- Y. Chen, X. Yang, Y. Cao, Z. Gan, and L. An, "Quantitative Study on Structural Evolutions and Associated Energetics in Polysilazane-Derived Amorphous Silicon Carbonitride Ceramics," *Acta Mater.*, **72** [15] 22–31 (2014).
- K. Wang, B. Ma, X. Li, Y. Wang, and L. An, "Effect of Pyrolysis Temperature on the Structure and Conduction of Polymer-Derived SiC," *J. Am. Ceram. Soc.*, **97** [7] 2135–8 (2014).
- Y. Chen, X. Yang, Y. Cao, and L. An, "Effect of Pyrolysis Temperature on the Electric Conductivity of Polymer-Derived Silicon Carbonitride," *J. Eur. Ceram. Soc.*, **34** [10] 2163–7 (2014).
- Y. Chen, F. Yang, and L. An, "On Electric Conduction of Amorphous Silicon Carbonitride Derived from a Polymeric Precursor," *Appl. Phys. Lett.*, **102**, 231902, 4pp (2013).
- K. Wang, B. Ma, Y. Wang, and L. An, "Complex Impedance Spectra of Polymer-Derived Silicon Oxycarbides," *J. Am. Ceram. Soc.*, **96** [5] 1363–5 (2013).
- C. Haluschka, C. Engel, and R. Riedel, "Silicon Carbonitride Ceramics Derived from Polysilazanes Part II. Investigation of Electrical Properties," *J. Eur. Ceram. Soc.*, **20** [9] 1365–74 (2000).
- P. Colombo, R. Riedel, G. D. Sorarù, and H.-J. Kleebe, *Polymer Derived Ceramics: From Nano-Structure to Applications*. DEStech Publications, Lancaster, Pennsylvania, 2010.
- Y. Wang, T. Jiang, L. Zhang, and L. An, "Optical Absorption in Polymer-Derived Amorphous Silicon Oxycarbonitrides," *J. Am. Ceram. Soc.*, **92** [12] 3111–3 (2009).
- Y. Wang, et al., "Effect of Thermal Initiator Concentration on the Electrical Behavior of Polymer-Derived Amorphous Silicon Carbonitrides," *J. Am. Ceram. Soc.*, **91** [12] 3971–5 (2008).
- H.-Y. Ryu, Q. Wang, and R. Raj, "Ultra-high-Temperature Semiconductors Made from Polymer-Derived Ceramics," *J. Am. Ceram. Soc.*, **93** [6] 1668–76 (2010).
- P. A. Ramakrishnan, et al., "Silicoboron-Carbonitride Ceramics: A Class of High-Temperature, Dopable Electronic Materials," *Appl. Phys. Lett.*, **78**, 3076, 3pp (2001).
- L. Liew, et al., "Ceramic MEMS-New Materials, Innovative Processing and Futuristic Application," *Am. Ceram. Soc. Bull.*, **80** [5] 25–30 (2001).
- X. Ren, S. Ebadi, Y. Chen, L. An, and X. Gong, "Characterization of SiCN Ceramic Material Dielectric Properties at High Temperatures for Harsh Environment Sensing Applications," *IEEE T. Microw Theory*, **61** [2] 960–71 (2013).
- Y. Li, Y. Yu, H. San, Y. Wang, and L. An, "Wireless Passive Polymer-Derived SiCN Ceramic Sensor with Integrated Resonator/Antenna," *Appl. Phys. Lett.*, **103**, 163505, 5pp (2013).
- H. Duan, C. Li, W. Yang, B. Lojewski, L. An, and W. Deng, "Near-Field Electro-spray Microprinting of Polymer-Derived Ceramics," *J. Microelectromech. S.*, **22** [1] 1–3 (2013).
- K. Wang, X. Li, B. Ma, Y. Wang, and L. An, "On Electronic Structure of Polymer-Derived Amorphous Silicon Carbide Ceramics," *Appl. Phys. Lett.*, **104**, 221902, 4pp (2014).
- K. Wang, B. Ma, X. Li, Y. Wang, and L. An, "Structural Evolutions in Polymer-Derived Carbon-Rich Amorphous Silicon Carbide," *J. Phys. Chem. A*, **119** [4] 552–8 (2015).
- Y. Wang, T. Jiang, L. Zhang, and L. An, "Electron Transport in Polymer-Derived Amorphous Silicon Oxycarbonitride Ceramics," *J. Am. Ceram. Soc.*, **92** [7] 1603–6 (2009).
- J. H. Simmons and K. S. Potter, *Optical Materials*. Academic Press, London, UK, 2000.
- S. K. J. Al-Ani and A. A. Higazy, "Study of Optical Absorption Edges in MgO-P₂O₅ Glasses," *J. Mater. Sci.*, **26** [13] 3670–4 (1991).
- A. Kumbhar, S. B. Patil, S. Kumar, R. Lal, and R. O. Dusan, "Photoluminescent, Wide-Bandgap a-SiC:H Alloy Films Deposited by Cat-CVD Using Acetylene," *Thin Solid Films*, **395** [1–2] 244–8 (2001).
- S. I. Andronenko, I. Stiharu, and S. K. Misra, "Synthesis and Characterization of Polyureasilazane Derived SiCN Ceramics," *J. Appl. Phys.*, **99**, 113907, 5pp (2006).
- P. O'Connor and J. Tauc, "Photoinduced Midgap Absorption in Tetrahedrally Bonded Amorphous Semiconductors," *J. Phys. Rev. B*, **25**, 2748–66 (1982).
- P. O'Connor and J. Tauc, "Spectrum of Photoinduced Optical Absorption in a-Si:H," *Solid State Commun.*, **36** [11] 947–9 (1980).
- J. C. Inkson, "Deep Impurities in Semiconductors: 11. The Optical Cross Section," *J. Phys. C: Solid State Phys.*, **14** [7] 1093–101 (1981).
- D. Pfost, H. Liu, Z. Vardeny, and J. Tauc, "Photoinduced Absorption Spectra in a-Ge:H and a-Si:H," *Phys. Rev. B*, **30**, 1083–6 (1984).
- X. Shi, H. Fu, J. R. Shi, L. K. Cheak, B. K. Tay, and P. Hui, "Electronic Transport Properties of Nitrogen Doped Amorphous Carbon Films Deposited by the Filtered Cathodic Vacuum Arc Technique," *J. Phys.: Condens. Matter*, **10** [41] 9293–302 (1998).
- M. Monthieux and O. Delverdier, "Thermal Behavior of (Organosilicon) Polymer-Derived Ceramics. V: Main Facts and Trends," *J. Eur. Ceram. Soc.*, **16** [7] 721–37 (1996).
- W. A. Nevin, H. Yamagishi, and Y. Tawada, "Wide Band-Gap Hydrogenated Amorphous Silicon Carbide Prepared from a Liquid Aromatic Carbon Source," *J. Appl. Phys.*, **72**, 4989, 3pp (1992).
- S. Trusso, F. Barreca, and F. Neri, "Bonding Configurations and Optical Band Gap for Nitrogenated Amorphous Silicon Carbide Films Prepared by Pulsed Laser Ablation," *J. Appl. Phys.*, **92**, 2485, 5pp (2002).
- J. Robertson, "The Electronic and Atomic Structure of Hydrogenated Amorphous Si-C Alloys," *Philos. Mag. B*, **66** [5] 615–38 (1992).
- M. M. Kamble, et al., "Hydrogenated Silicon Carbide Thin Films Prepared with High Deposition Rate by Hot Wire Chemical Vapor Deposition Method," *J. Coating*, **2014**, 905903, 11pp (2014).

⁴⁰A. M. Hermann, et al., "Structure and Electronic Transport Properties of Si-(B)-C-N Ceramics," *J. Am. Ceram. Soc.*, **84** [10] 2260–4 (2001).

⁴¹G. Mera, A. Navrotsky, S. Sen, H.-J. Kleebe, and R. Riedel, "Polymer-Derived SiCN and SiOC Ceramics – Structure and Energetics at the Nanoscale," *J. Mater. Chem. A*, **1**, 3826–36 (2013).

⁴²N. F. Mott, "Conduction in Glasses Containing Transition Metal Ions," *J. Non-Cryst. Solids*, **1** [1] 1–17 (1968).

⁴³N. F. Mott, "Conduction in Non-Crystalline Materials III. Localized States in a Pseudogap and Near Extremities of Conduction and Valence Bands," *Philos. Mag.*, **19** [160] 835–52 (1969).

⁴⁴C. Godet, "Physics of Bandtail Hopping in Disordered Carbons," *Diamond Relat. Mater.*, **12** [2] 159–65 (2003).

⁴⁵C. Godet, "Hopping Model for Charge Transport in Amorphous Carbon," *Philos. Mag. B*, **81** [2] 205–22 (2001). □